# Characteristic Excitation Taper for Ultrawideband Tightly Coupled Antenna Arrays

Ioannis Tzanidis, *Member, IEEE*, Kubilay Sertel, *Senior Member, IEEE*, and John L. Volakis, *Fellow, IEEE*

***Abstract*—We propose a novel technique to calculate a quasi-optimal aperture excitation for finite size, ultrawideband arrays. The approach is based on using the characteristic modes of the array's mutual impedance matrix. Unlike standard excitation tapers, primarily used for beam shaping, the proposed characteristic mode taper provides for wideband matching of all array elements, including those at the edges of the finite array. As such, it maximizes aperture efficiency and is particularly attractive for finite size, tightly coupled antenna arrays. Our method solely relies on the $N \times N$ mutual impedance matrix of the array which is precomputed (or measured). We demonstrate this novel excitation method for an $8 \times 8$ array of tightly coupled dipole elements. When compared to uniform excitation, the characteristic mode excitation achieves very low $VSWRs$ for all elements over a large bandwidth. Improvements in realized gain are also demonstrated. Due to its simplicity, this new method can be incorporated into a design process to optimize element and array geometries, leading to further performance improvements.**

***Index Terms*—Characteristic modes, current sheet array, finite arrays, impedance matching, phased arrays, tightly coupled arrays, ultrawideband arrays.**

## I. Introduction

NEW generation communication devices and imaging radars require larger bandwidths to transmit high-data-rates and obtain high quality images. Very often, these systems must also operate at high power. These requirements imply antennas that are ultrawideband, well matched, and of high gain. Of equal importance is that the antenna size and thickness remain relatively small compared to the wavelength for conformal installations. To this end, arrays of tightly coupled dipoles ([1], [2]) were recently shown to provide very wide impedance bandwidth (>5:1) even when installed close to a metallic surface. For this reason, tightly coupled arrays are very attractive for application in the aforementioned systems.

An example of a tightly coupled array is the overlapping dipole array shown in Fig. 1. This simple topology achieves a continuous ~5:1 bandwidth coverage, even though its overall thickness is only $\lambda/10$ at the lowest operational frequency. As depicted, the array consists of dipole elements coupled with their nearest neighbors at their tips, via a capacitive overlapping section. This capacitive coupling counteracts the inductive effects of the ground plane, realizing wideband operation [3]. In an infinite array setting, each element of this topology (i.e., unit cell) has a very simple circuit model that greatly facilitates array design [1].

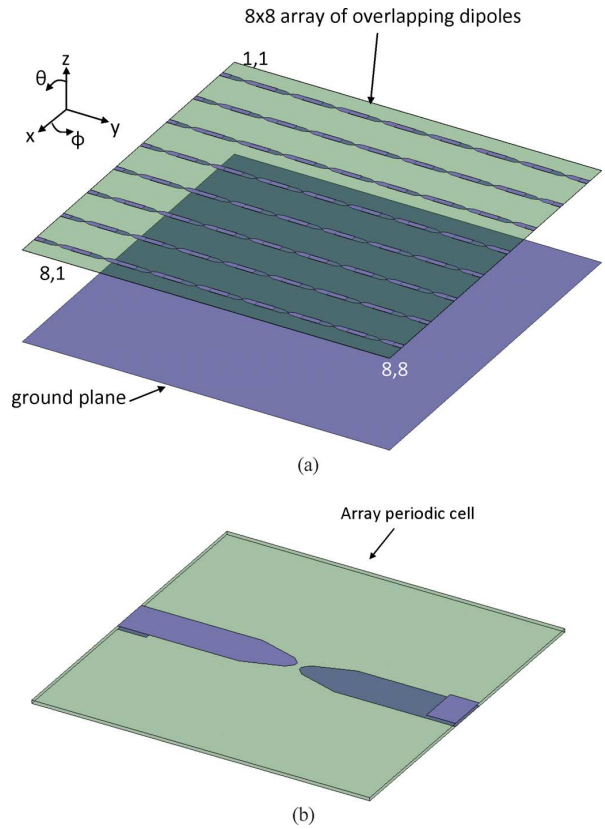


Fig. 1. (a) $8 \times 8$ element array of overlapping dipoles above a ground plane. (b) A detail from its unit cell.

Although the infinite array approach provides for a computationally fast analysis (since only a single unit cell is modeled using periodic boundary conditions), it does not account for finite array edge effects. Specifically, for finite size arrays, edge and corner diffraction effects render the outer periphery elements mismatched. As a result, the impedance of the edge and corner elements within a finite size array, usually differs significantly from the intended design (infinite array). Thus, the finite array bandwidth is degraded and several costly redesign steps are required to achieve the intended operation.

A technique to alleviate this is to simply not excite (i.e. resistively terminate as in [2], [4]–[6]) the periphery elements and excite uniformly only the central portion of the array. This approach obviously reduces aperture efficiency significantly. Another approach to suppress edge effects is to redesign the elements close to the array edges. However, for medium to large

Manuscript received June 30, 2011; revised September 01, 2011; accepted October 26, 2011. Date of publication January 31, 2012; date of current version April 06, 2012.

The authors are with the ElectroScience Lab., The Ohio State University, Columbus, OH 43212 USA (e-mail: tzanidis.1@osu.edu; url: http://electroscience.osu.edu/8794.cfm).

Color versions of one or more of the figures in this paper are available online at http://ieeexplore.ieee.org.

Digital Object Identifier 10.1109/TAP.2012.2186269

size arrays, this approach is very costly as it requires large computational resources. That is, achieving impedance matching for all elements in a finite array and over a broad frequency range is not a trivial task.

A straightforward approach to achieve good active-impedance matching for all array elements is to employ different excitation for each element. However, without a clear guidance on how to choose each element's excitation, this method is impractical.

In this paper, we present a method to design the excitation taper of finite size tightly coupled arrays for efficient matching of all array elements. The proposed method is based on the characteristic modes (CMs) associated with the mutual impedance matrix of the finite array. It is shown that the characteristic mode excitation leads to perfect impedance matching for all array elements, albeit only at a single frequency. Nonetheless, the impedance behavior over an extended frequency band is still favorable. Thus, the CM excitation can be considered as a quasi-optimal solution to the $N$-port wideband matching problem. Further optimizations can, of course, be carried out starting with the CM taper to improve impedance bandwidth.

The theory of characteristic modes was introduced by Garbacz [7], [8] and Harrington [9]–[13] and the reader is referred to any one of these papers for its basic principles. One of the important features of the CM technique is that it can incorporate the platform effects on which the array is mounted on.

Different array excitation tapers have been previously devised for side-lobe/beamwidth control [14] and for improving the directivity of narrowband [15], [16] and broadband arrays [17]. Also, characteristic modes and the similar Inagaki modes [18] have previously been applied to synthesize array patterns [19], [20]. Designs of reconfigurable antennas based on CMs were reported [21] as well. However, this is the first time that the CM theory is employed to design the excitation of broadband arrays for near-optimal impedance matching and improved gain.

The paper is organized as follows: Section II reviews the key aspects of the CM theory and its adoption to finite array excitation design. Section III illustrates the proposed array excitation technique applied to an $8 \times 8$ array of overlapping dipoles. Section IV provides numerical results for the realized gain and radiation patterns of the dipole array when excited with the CM taper. Comparison to the uniformly excited aperture is also given to assess the CM-based design.

## II. Characteristic Mode Excitation of Finite Tightly Coupled Arrays

### A. A Brief Review of Characteristic Mode Theory

As already noted, the theory of CMs is presented in [7]–[13], [22] for conductive and dielectric bodies. For perfect electrically conducting (PEC) bodies the CMs correspond to fields associated with the $N$ eigenvectors (or eigencurrents) $\{I\}$ of the generalized eigenvalue problem

$$[X]\{I\} = \lambda[R]\{I\} \tag{1}$$

where

$$[Z] = [R] + j[X], \tag{2}$$

is the $N \times N$ moment method impedance matrix of the structure at frequency $f$ and $\lambda$ are the usual eigenvalues. We remark, that throughout the paper, vector quantities are denoted by $\{\cdot\}$, and matrices by $[\cdot]$.

Obviously, from (2), $[R]$ and $[X]$ correspond to the real and imaginary parts of the impedance matrix, respectively. As the impedance matrix $[Z]$ is complex symmetric, both $[R]$ and $[X]$ are also symmetric and real matrices. As a consequence, the eigenvalues and eigenvectors of (1) are all real. Also, $[R]$ is positive definite for open-surfaces.

When an eigenvalue $\lambda_k$ is near zero at a certain frequency $f$, the CM $\{I_k\}$ is said to be at *resonance*, implying $[X]\{I_k\} \approx 0$. The fact that $[X]\{I_k\} \approx 0$ for a CM close to resonance is key to the proposed CM aperture excitation. However, before we go into details, the following property of the CMs is noteworthy; namely, the eigencurrents $\{I\}$ obey the generalized orthogonality relationship

$$\tilde{I}_m^*[R]I_n = \delta_{mn}. \tag{3}$$

Here, the asterisk denotes complex conjugate, the tilde denotes transpose, and $\delta_{mn}$ is Kronecker's delta. This property is used later on to numerically distinguish modes from each other.

As mentioned in [22], characteristic modes can also be defined in terms of an $N$-port network using the $N \times N$ mutual impedance matrix $[Z_S]$. The CMs of the network can be found from (1) by just replacing $[Z]$ with $[Z_S]$. For our antenna study, the $N$-port network is simply comprised of the $N$ elements of the tightly coupled array. Below, we illustrate how the CM theory is applied to calculate the excitation taper for finite size wideband arrays, resulting in a minimum reflection at all ports.

### B. Characteristic Mode Based Excitation of Finite Arrays

As noted above, the CMs for a general $N$-port network are simply the eigenvectors of the mutual impedance matrix. For a finite array of $N$ elements as the one shown in Fig. 2, the $N$-port impedance matrix $[Z_S]$ can be used in (1) to extract $\{I_k\}$. Since $[Z_S]$ is symmetric with $[R_S]$ being positive definite, then $\{I_k\}$ are real. Further, when the eigenmodes $\{I_k\}$ corresponding to $\lambda_k \approx 0$ are used to excite the array, the induced port voltages $\{V_k\}$ are also real and in phase with the excitation. That is

$$\begin{aligned}\{V_k\} &= [Z_S]\{I_k\} \\ &= [R_S]\{I_k\} + j[X_S]\{I_k\} \\ &= [R_S]\{I_k\} + j\lambda_k[R_S]\{I_k\} \\ &\approx [R_S]\{I_k\}.\end{aligned} \tag{4}$$

From (4) the active impedance $\{Z_a\}$ for the array elements can then be expressed as

$$\{Z_a\} = \{V_k\}./\{I_k\} \rightarrow [R_S]\{I_k\}./\{I_k\}. \tag{5}$$

Here, "./" denotes element-wise division between the two vectors. We also note that since both $\{V_k\}$ and $\{I_k\}$ are real valued, the resulting active port impedances are also real. Consequently, all array ports can now be matched simultaneously, provided each port is fed by a transmission line having a characteristic impedance equal to the active port impedance.

Although the above procedure leads to optimal current excitation, it is more appropriate to calculate the *incident power* excitation taper as the $S$-parameters are more appropriate for evaluating matching performance. Before we proceed to do so, we must first address the following subtleties.

So far, CMs were calculated and used at a single frequency. However, for arrays, we are interested in wideband matching. But as the eigenvalues are frequency dependent, purely resistive active impedance may not be achieved over a wide bandwidth. Thus, the frequency behavior of the CMs needs be assessed prior to using the CM method as guidance for feed excitations.

With the above concerns in mind, we can proceed to introduce the *mode significance* parameter $\alpha$ [9]

$$\alpha = \frac{1}{1+|\lambda|}. \tag{6}$$

This simple expression maps the range of CM eigenvalues $\lambda \in (0, +\infty)$ to the interval (0, 1), making it convenient for plotting. It will be later demonstrated that the range of frequencies for which $0.6 \leq \alpha \leq 1$ provides for an empirical way to estimate the array bandwidth. Below we illustrate the relevance of the modal significance parameter $\alpha$.

Consider a coupled dipole array of size $D \times D$ above a ground plane as in Fig. 2(a). A typical plot of the mode significance $\alpha$ vs. frequency for such an array is given in Fig. 2(b), for the first 5 dominant modes. As seen, each CM either resonates around $D \approx \lambda/2$ or $D \approx \lambda$ or both. Indeed, ordinary resonances occur when the linear aperture size $D$ is multiples of a half-wavelength. The corresponding current distributions on the array at resonance are also illustrated in Fig. 2(a), using the same color and line style.

We observe that among the 5 CMs shown in Fig. 2(b), mode 1 (solid curve) is observed to exhibit the largest frequency span, where $\alpha > 0.6$. Hence, the eigencurrent corresponding to mode 1 is a good choice for guiding aperture excitation. From Fig. 2(a)), we see that mode 1 has sinusoidal current distributions along the dipole lengths and almost uniform in the transverse direction.

The corresponding radiation patterns of modes 1 to 5 are simply found by the 2D Fourier Transform of the mode currents [23]. However, as the finite ground plane affects radiation, the actual pattern must be computed after the final excitation is calculated. Nonetheless, the CM radiation pattern (see Fig. 2(c)), is an other criterion for selecting among the different CMs. Indeed, from Fig. 2(c), we observe that mode 1 is associated with a broadside radiation pattern. In contrast, modes 3–5 give end-fire patterns. Also, mode 2 gives a more directive pattern than mode 1. Thus, it terms of bandwidth and pattern mode 1 is the best choice to guide the array excitation.

The next step in the procedure is to calculate the excitation coefficients $a_i$ for the incident power waves, and the input line impedances $Z_{0i}$, for each array element. As summarized below, $a_i$ can be readily found using the standard definitions of the $S$-parameters [24]. Namely we have

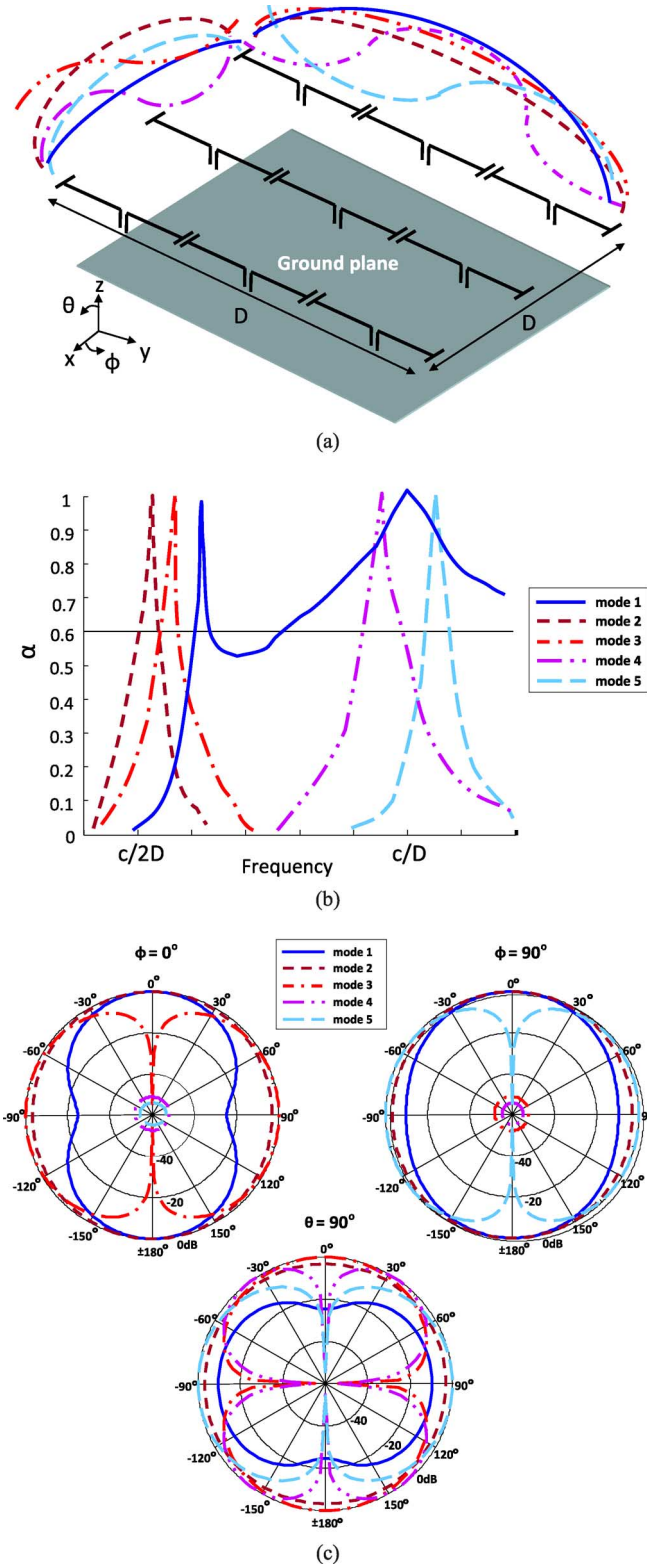


Fig. 2. (a) Tightly coupled dipole array over a ground plane and associated mode current distributions at the resonance frequencies. (b) Typical modal significance plots for the array in Fig. 2(a); modes resonate approximately at the frequencies where aperture size $D$ is multiples of half-wavelengths. (c) Radiation patterns corresponding to modes 1 to 5 at $\phi = 0°, 90°$ and $\theta = 90°$ cuts (see Fig. 1 for axes).

and

$$[Z_0]^{-0.5}\{V_1\} = \{a\} + \{b\}, \tag{7}$$

$$[Z_0]^{0.5}\{I_1\} = \{a\} - \{b\}, \tag{8}$$

where $\{a\}$ and $\{b\}$ contain the coefficients $a_i$ and $b_i$ for the incident and reflected waves, respectively, at the $i^{th}$ element. Also, $[Z_0]$ is a diagonal matrix containing the characteristic impedances of the feeding lines, $\{I_1\}$ is the current associated with mode 1 at the port location, and $\{V_1\}$ is calculated from (4). By adding (7) and (8) we can obtain the CM excitation coefficients, viz.

$$\{a\} = 0.5[Z_0]^{-0.5}\{V_1\} + 0.5[Z_0]^{0.5}\{I_1\}. \tag{9}$$

In addition, the entries of the diagonal matrix $[Z_0]$ are found from

$$[Z_0] = |\{V_1\}./\{I_1\}|\,. \tag{10}$$

where, as before, "./" denotes element-wise division between the two vectors. These coefficients and line impedances form the excitation taper that will be used to feed the array elements. Of course, the above distribution is computed at a single frequency (CM resonance frequency) within the operational bandwidth. We will see later that the optimal choice of that frequency depends on the final performance of the array when the computed excitation taper is applied.

In general, the wave excitations $a_i$ are complex. In our realization though, we choose $|\{a\}|$. Nevertheless, this choice does not affect matching significantly since $\{a\}$ and $[Z_0]$ are computed for CMs close to resonance. Indeed, as was shown in (4), at resonance $\{V\}$ and $\{I\}$ are real, as well as $[Z_0]$ and hence $\{a\}$. The computed coefficients $|\{a\}|$ and line impedances $[Z_0]$ are used as constant for all frequencies.

The reflected wave coefficients $\{b\}$ can be computed using the $N$-port $S$-parameter matrix $[S_S]$ of the array found from

$$[S_S] = [Z_0]^{-0.5}\left([Z_S] - [Z_0]\right)\left([Z_S] + [Z_0]\right)^{-1}[Z_0]^{0.5}. \tag{11}$$

Subsequently, the magnitude of the active reflection coefficient $\Gamma$, and the active $VSWR$ at each port can readily be computed via

$$\{b\} = [S_S]\,|\{a\}|\,, \tag{12}$$

$$|\{\Gamma\}| = |\{b\}./|\{a\}||\,, \tag{13}$$

$$\{VSWR\} = \left(1 + |\{\Gamma\}|\right)./\left(1 - |\{\Gamma\}|\right). \tag{14}$$

Given $\{a\}$ and $\{b\}$, we can also evaluate the mismatch efficiency of the system, $e_{mis}$, from

$$e_{mis} = \frac{\sum |a_i|^2 - \sum |b_i|^2}{\sum |a_i|^2}100\%. \tag{15}$$

Below, we present an example of the excitation procedure outlined above. Specifically, an 8 × 8 element array of coupled dipoles is employed. This array operates in the 200–600 MHz band and is placed 6″ above a ground plane.

## III. Finite Array of Overlapping Dipoles Over a Ground Plane

To illustrate the CM excitation method for UWB arrays, an 8 × 8 array of overlapping dipoles, shown in Fig. 1, is considered. The overall size of the planar array is 2′ × 2′ and is placed 6″ above a 2′ × 2′ ground plane.

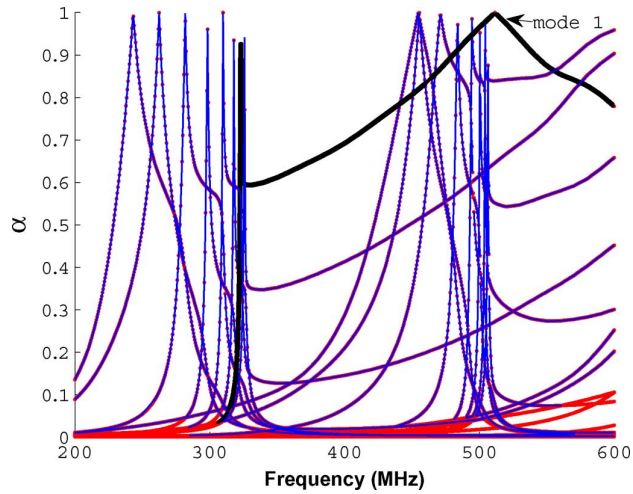


Fig. 3. Mode significance plot for the array depicted in Fig. 1(a).

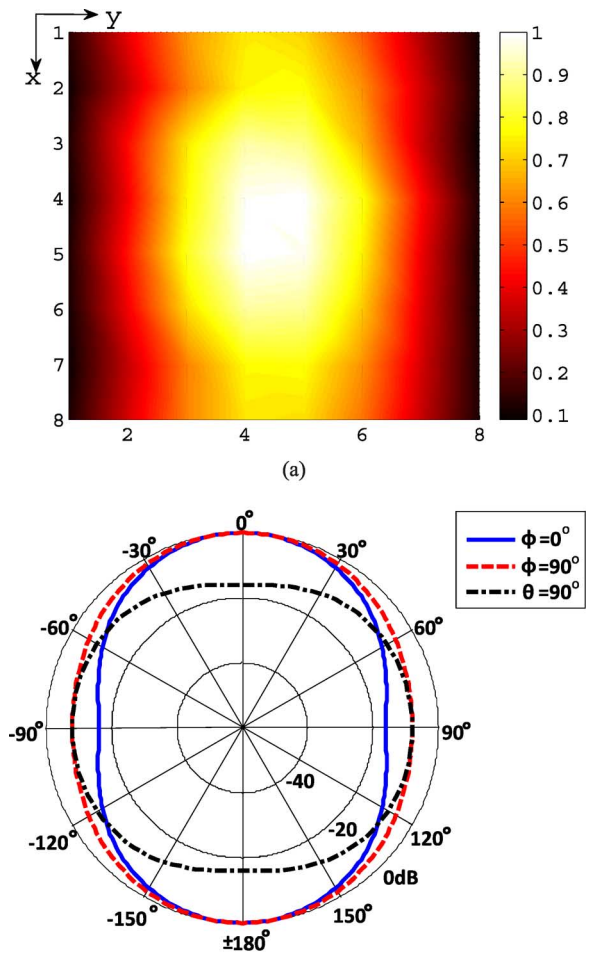


Fig. 4. (a) Current distribution of mode 1 at 511 MHz (white refers to strongest and dark to lowest values); element numbering is shown in Fig. 1. (b) Mode 1 radiation pattern at $\phi = 0°, 90°$ and $\theta = 90°$ cuts (see Fig. 1 for axes).

As first step to design the excitation, the entire array was analyzed using HFSS ver.12. The 64 × 64 mutual impedance matrix $[Z_S]$ of the array was obtained at a discrete set of frequencies in the 200–600 MHz range. Subsequently, the eigenvalue problem (1) was solved to obtain modal significance parameter

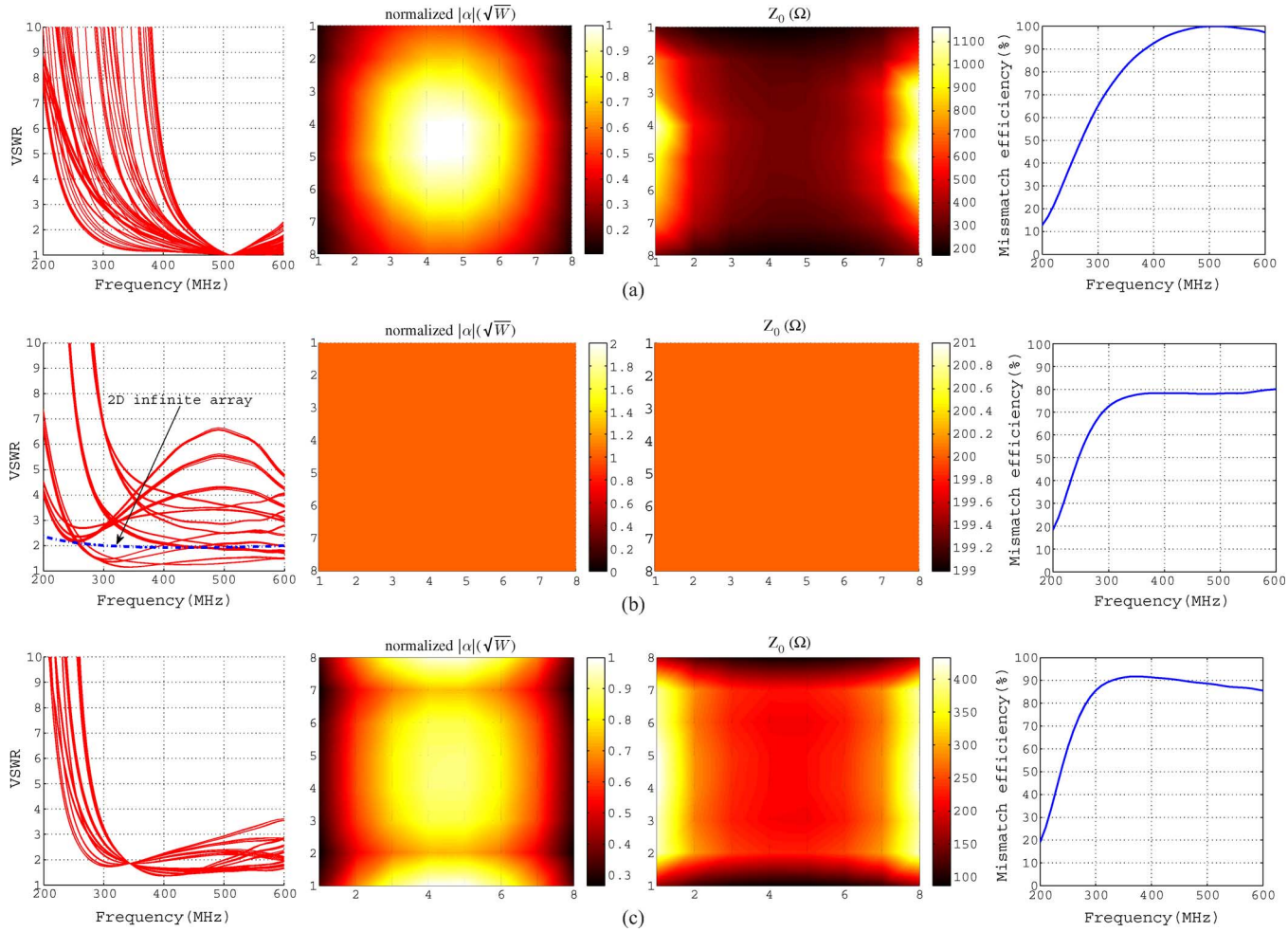


Fig. 5. (left to right) Active $VSWR$ for all array elements, excitation coefficients, line impedances, and mismatch efficiency. (a) Excitation taper calculated based on current distribution of mode 1 at 511 MHz. (b) Uniform excitation. (c) Excitation taper calculated based on current distribution of mode 1 at 343.5 MHz (element numbering is shown in Fig. 1).

$\alpha$. The latter is plotted in Fig. 3. As highlighted in Fig. 3, mode 1 becomes significant ($\alpha \geq 0.6$) above 325 MHz and resonates at 511 MHz. The current distribution and radiation patterns corresponding to this mode are shown in Fig. 4. It is clear that this mode is an excellent choice to guide the feed distribution for broadband operation.

Using the CM excitation process described above, we proceeded to calculate the excitation coefficients $|a|$, characteristic impedances $Z_0$ of feed lines, active $VSWR$, and mismatch efficiency for each individual elements. Of particular interest is the active $VSWR$ at each array element, depicted in the leftmost column of Fig. 5(a). When the current associated with mode 1 at 511 MHz is used as the array's excitation taper, all array elements become matched at that frequency. This is clear from Fig. 5(a). We also note that the efficiency drops at lower frequencies. This was to be expected as the impedance mismatch increases significantly as the aperture becomes smaller. For comparison, we also present the corresponding performance for a uniformly aperture excitation $\{a\} = \{1\}$, with $Z_0 = 200\ \Omega$ for all elements. As seen, all array elements exhibit significant mismatches across the band. This should be contrasted with the original infinite array $VSWR$ performance which is also given in Fig. 5(b). The severe mismatch caused by the finite array truncation is clearly demonstrated.

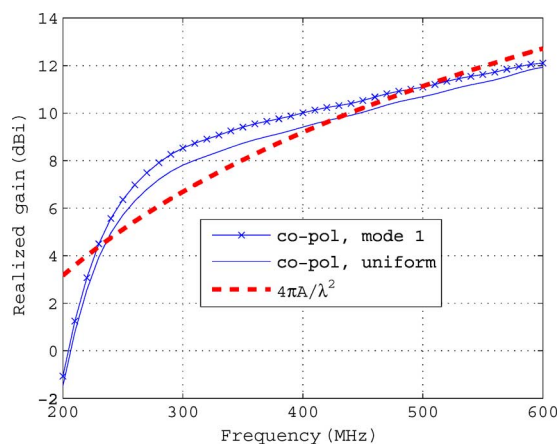


Fig. 6. Realized gain of the array shown in Fig. 1(a) for the excitations shown in Fig. 5(c) and 5(b). The directivity of a uniformly illuminated rectangular aperture of area $A = 2' \times 2'$ on an infinite PEC ground plane is also plotted.

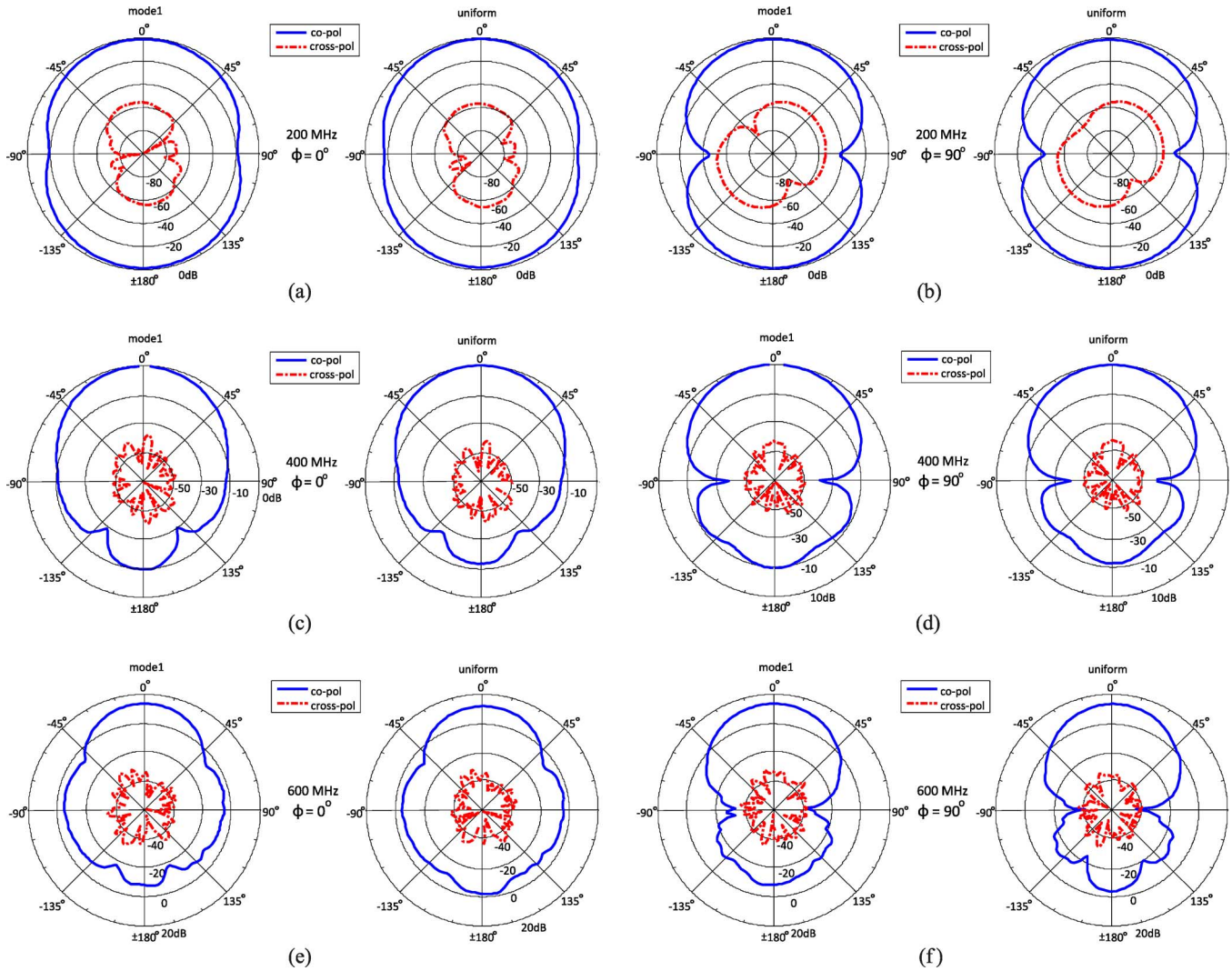


Fig. 7. Radiation patterns of the array shown in Fig. 1(a) when excited using the mode 1 taper shown in Fig. 5(c) and the uniform excitation shown in Fig. 5(b). (a) Pattern at 200 MHz, $\phi = 0^\circ$ plane. (b) Pattern at 200 MHz, $\phi = 90^\circ$ plane. (c) Pattern at 400 MHz, $\phi = 0^\circ$ plane. (d) Pattern at 400 MHz, $\phi = 90^\circ$ plane. (e) Pattern at 600 MHz, $\phi = 0^\circ$ plane. (f) Pattern at 600 MHz, $\phi = 90^\circ$ plane.

The proposed CM excitation (Fig. 5(a)) results in simultaneous impedance match for all array elements at the CM resonant frequency of 511 MHz. Nonetheless, the overall impedance bandwidth for active $VSWR < 3$ is not large enough to accommodate UWB operation.

This shortcoming can be alleviated if the CM resonance condition $\alpha = 1$ is relaxed to $\alpha = 0.6$. As mentioned above, $\alpha = 1$ corresponds to $VSWR = 1$ for all elements, albeit for a small bandwidth. Relaxing the modal significance parameter to $\alpha = 0.6$ corresponds to relaxing the impedance match condition to $VSWR = 2$ for all elements. In turn, greater bandwidth is achieved. With this in mind, the excitation is calculated based in the CM current at $f = 343.5$ MHz. Indeed, a much better $VSWR$ performance is achieved as depicted in Fig. 5(c). The overall active impedance bandwidth (for $VSWR < 3$) can now cover the entire 300–600 MHz for all elements (except 4 at the top and bottom edges of the array, viz. elements (1, 4), (1, 5), (8, 4), and (8, 5) (see Fig. 1 for element enumeration). Reference port impedances (i.e. characteristic impedances of feed lines) shown in the third column of Fig. 5(c) are also found as a result of the CM analysis.

Fig. 5 also shows are the mismatch efficiency for the corresponding excitation tapers. These curves are computed assuming an ideal power divider/combiner for all 64 ports. As indicated, the overall mismatch efficiency is approximately the same for all three excitation tapers. Thus, it might seem that the benefit of using the proposed CM taper is inconsequential. However, in reality this plot simply accentuates the fact that a very high system efficiency (even as much as 80% in the uniform excitation case), can still hide the fact that a significant number of elements may be mismatched.

Below, we present the performance of the array for the chosen excitation using full-wave simulations.

## IV. Performance Validation using Full-Wave Simulations

To further demonstrate the validity of the proposed excitation design method, we present full-wave simulation data for the

simple array shown in Fig. 1(a). The element geometry was initially designed for optimal performance within an infinite array and then used to create an $8 \times 8$ finite array. As already noted the finite array was excited using the CM taper and the feed-line impedances given in Section III (see Fig. 5(c)). For comparison, the same array was also excited uniformly using 200 $\Omega$ feed lines.

The realized array gain (co-polarized component) at broadside ($\theta = 0^\circ$) is shown in Fig. 6 for the CM taper and uniform excitation. Also, the directivity of a uniformly excited rectangular aperture of area $A = 2' \times 2'$ (situated on an infinite PEC ground plane) is shown for [23]. As observed, the CM taper provides an additional 1 dB gain over the uniform excitation. This improvement is obviously due to the improved impedance match of the array elements. We should also note that the cross-polarized isolation for both excitations (uniform and CM-based) is $\sim$50 dB throughout the whole band.

The radiation patterns of the $8 \times 8$ array at 200, 400 and 600 MHz and at the $\phi = 0^\circ$, $90^\circ$ planes are shown Fig. 7. Similar radiation patterns are obtained for the two excitations.

We note that the simulated active $VSWRs$ obtained from HFSS, were found to be precisely equal to those given in Fig. 5(b) and 5(c) for all elements and both excitation tapers (uniform and CM-based). Therefore these plots were omitted.

## V. Conclusions and Discussion

We proposed a simple, yet effective, aperture excitation technique for finite size UWB tightly coupled antenna arrays. To achieve much improved active impedance match at all $N$ array elements, we consider the CMs of the $N \times N$ mutual coupling matrix. When CM current distributions are used as the array excitation, the optimal feed-line impedances can also be calculated. As compared with the standard uniform excitation, the CM excitation technique provides optimum impedance matching, simultaneously for all array elements over a broad range of frequencies.

We remark that the CM excitation technique is more applicable to arrays with strong mutual coupling. For weakly coupled arrays, the mutual impedance matrix is almost diagonal and it is therefore possible that the element resonances dominate. As such, the CMs may no longer be associated with the radiating aperture size. In contrast, in the case of strong mutual coupling, the array behaves much like a single radiating aperture. Therefore, the characteristic modes of the array's mutual impedance matrix will be associated with the whole aperture and not the individual elements.

We demonstrated that this novel technique also improves realized array gain. Specifically, a 0.5–1 dB additional gain was obtained for a simple $8 \times 8$ coupled dipole array. Continuous 300–600 MHz bandwidth coverage was also demonstrated for the VSWR.

This simple approach can also be implemented into exciting array structures using the *measured* mutual impedance matrix. Particularly for high power arrays, the simultaneous matching of all array elements is of utmost importance.

## VI. Symbols

| | |
|---|---|
| $[Z]$ | moment method impedance matrix |
| $[R]$ | real part of moment method impedance matrix |
| $[X]$ | imaginary part of moment method impedance matrix |
| $\{I\}$ | eigencurrent associated with a characteristic mode |
| $\lambda$ | eigenvalue associated with a characteristic mode |
| $[Z_S]$ | mutual impedance matrix of $N \times N$ array |
| $[R_S]$ | real part of mutual impedance matrix |
| $[X_S]$ | imaginary part of mutual impedance matrix |
| $\{I_k\}$ | total current at dipoles's feed points. This is the eigencurrent of mode $k$ |
| $\{V_k\}$ | total voltage at dipoles's feed points corresponding to current $\{I_k\}$ |
| $\lambda_k$ | eigenvalue associated with characteristic mode $k$ at a given frequency |
| $\{Z_a\}$ | active impedance of all array elements |
| $\alpha$ | modal significance parameter associated with mode eigenvalues |
| $[Z_0]$ | diagonal matrix containing feed line characteristic impedances |
| $\{a\}$ | incident waves at feed ports of array |
| $\{b\}$ | reflected waves at feed ports of array |
| $[S_S]$ | scattering matrix of $N \times N$ array |
| $\{\Gamma\}$ | reflection coefficient at feed ports of array |
| $\{VSWR\}$ | voltage standing wave ratio at feed lines of array |
| $e_{miss}$ | total mismatch efficiency of array |

## References


[1] B. Munk, *Finite Antenna Arrays and FSS*. Piscataway-Hoboken, NJ: Wiley-IEEE Press, 2005.

[2] M. Jones and J. Rawnick, "A new approach to broadband array design using tightly coupled elements," in *Proc. IEEE MILCOM*, Oct. 29–31, 2007, pp. 1–7.

[3] J. L. Volakis and K. Sertel, "Narrowband and wideband metamaterial antennas based on degenerate band edge and magnetic photonic crystals," *Proc. IEEE*, vol. 99, no. 10, pp. 1732–1745, 2011.

[4] I. Tzanidis, K. Sertel, and J. Volakis, "Excitation and termination of finite tightly coupled antenna arrays based on structural characteristic modes," presented at the Antenna Applications Symp., 2011.

[5] J. Lee, S. Livingston, and R. Koenig, "A low-profile wide-band (5:1) dual-pol array," *IEEE Antennas Wireless Propag. Lett.*, vol. 2, pp. 46–49, 2003.

[6] H. Holter, "Dual-polarized broadband array antenna with BOR-elements, mechanical design and measurements," *IEEE Trans. Antennas Propag.*, vol. 55, no. 2, pp. 305–312, Feb. 2007.

[7] R. Garbacz, "A Generalized Expansion for Radiated and Scattered Fields," Ph.D. dissertation, The Ohio State Univ., Columbus, 1968.

[8] R. Garbacz and R. Turpin, "A generalized expansion for radiated and scattered fields," *IEEE Trans. Antennas Propag.*, vol. 19, no. 3, pp. 348–358, May 1971.

[9] R. Harrington and J. Mautz, "Theory of characteristic modes for conducting bodies," *IEEE Trans. Antennas Propag.*, vol. 19, no. 5, pp. 622–628, Sep 1971.

[10] R. Harrington and J. Mautz, "Computation of characteristic modes for conducting bodies," *IEEE Trans. Antennas Propag.*, vol. 19, no. 5, pp. 629–639, Sep 1971.
[11] R. Harrington, J. Mautz, and Y. Chang, "Characteristic modes for dielectric and magnetic bodies," *IEEE Trans. Antennas Propag.*, vol. 20, no. 2, pp. 194–198, Mar 1972.
[12] J. Mautz and R. Harrington, "Modal analysis of loaded n-port scatterers," *IEEE Trans. Antennas Propag.*, vol. 21, no. 2, pp. 188–199, Mar 1973.
[13] R. Harrington and J. Mautz, "Control of radar scattering by reactive loading," *IEEE Trans. Antennas Propag.*, vol. 20, no. 4, pp. 446–454, July 1972.
[14] C. Dolph, "A current distribution for broadside arrays which optimizes the relationship between beam width and side-lobe level," *Proc. IRE*, vol. 34, no. 6, pp. 335–348, 1946.
[15] D. Cheng and F. Tseng, "Gain optimization for arbitrary antenna arrays," *IEEE Trans. Antennas Propag.*, vol. 13, no. 6, pp. 973–974, Nov. 1965.
[16] C. Tai, "The optimum directivity of uniformly spaced broadside arrays of dipoles," *IEEE Trans. Antennas Propag.*, vol. 12, no. 4, pp. 447–454, July 1964.
[17] C. Sharpe and R. Crane, "Optimization of linear arrays for broadband signals," *IEEE Trans. Antennas Propag.*, vol. 14, no. 4, pp. 422–427, July 1966.
[18] N. Inagaki and R. Garbacz, "Eigenfunctions of composite hermitian operators with application to discrete and continuous radiating systems," *IEEE Trans. Antennas Propag.*, vol. 30, no. 4, pp. 571–575, Jul. 1982.
[19] R. Harrington and J. Mautz, "Pattern synthesis for loaded n-port scatterers," *IEEE Trans. Antennas Propag.*, vol. 22, no. 2, pp. 184–190, Mar. 1974.
[20] D. Pozar, "Antenna synthesis and optimization using weighted inagaki modes," *IEEE Trans. Antennas Propag.*, vol. 32, no. 2, pp. 159–165, Feb. 1984.
[21] K. Obeidat, B. Raines, R. Rojas, and B. Strojny, "Design of frequency reconfigurable antennas using the theory of network characteristic modes," *IEEE Trans. Antennas Propag.*, vol. 58, no. 10, pp. 3106–3113, 2010.
[22] , R. Mittra, Ed., *Numerical and Asymptotic Techniques in Electromagnetics*, ser. Topics in Applied Physics. Berlin: Springer, 1975, vol. 3, ch. 3, pp. 51–87.
[23] , C. Balanis, Ed., *Antenna Theory: Analysis and Design*, 3rd ed. New York: Wiley-Interscience, 2005, ch. 12, pp. 653–738.
[24] P. Young, "Scattering coefficients and circuit analysis," in *Proc. 14th IEE Microwave Measurements Training Course*, May 2005, pp. 2–2/11, (Ref. No. 2005/10870).

**Ioannis Tzanidis** (M'11) was born in 1983. He received the Diploma in Electrical and Computer Engineering from Democritus University of Thrace, Xanthi, Greece and the M.Sc. and Ph.D. degrees from the Ohio State University, Columbus, in 2010 and 2011, respectively.

He currently works as a Postdoctoral Researcher at the ElectroScience Laboratory, Ohio State University. His research interests include wideband antennas, antenna miniaturization techniques, UWB arrays, array feeding techniques, and MIMO antennas.

Dr. Tzanidis received the 1st place in the student paper competition at the 2010 Antennas and Propagation Symposium, one of the most prestigious student paper awards in the world.

**Kubilay Sertel** (SM'07) received the Ph.D. degree from the University of Michigan at Ann Arbor, in 2003.

He is currently a Research Scientist at the ElectroScience Laboratory and an Adjunct Professor at the Electrical and Computer Engineering Department, Ohio State University, Columbus. His research areas include analysis and design of ultra wideband antennas and arrays, reconfigurable antennas and arrays and miniaturization techniques, THz sensors and sensor arrays for medical and non-destructive imaging, metamaterials and frequency selective surfaces/volumes, and measurement and characterization of anisotropic and magneto-dielectric composites, applied computational electromagnetics, integral equation methods, fast and efficient modeling of large-scale, real-life electromagnetics problems on massively parallel computing platforms. He coauthored the books *Frequency Domain Hybrid Finite Element Methods in Electromagnetics* (Morgan & Claypool, 2006), and *Integral Equation Methods for Electromagnetics* (SciTech Publishing, 2012) and published over 40 journal papers and 170 conference articles.

Dr. Sertel an elected member of URSI Commission B, and a member of Applied Computational Electromagnetics Society.

**John L. Volakis** (S'77–M'82–SM'89–F'96) was born on May 13, 1956 in Chios, Greece and immigrated to the U.S.A. in 1973. He received the B.E. degree (*summa cum laude*) from Youngstown State University, Youngstown, OH, in 1978, and the M.Sc. and Ph.D. degrees from the Ohio State University, Columbus, in 1979 and 1982, respectively.

He started his career at Rockwell International (1982–1984), now Boeing Phantom Works. In 1984, he was appointed Assistant Professor at the University of Michigan, Ann Arbor, becoming a full Professor in 1994. He also served as the Director of the Radiation Laboratory from 1998 to 2000. Since January 2003, he is the Roy and Lois Chope Chair Professor of Engineering at the Ohio State University, Columbus, and also serves as the Director of the ElectroScience Laboratory. His primary research deals with antennas, computational methods, electromagnetic compatibility and interference, propagation, design optimization, RF materials, multi-physics engineering and bioelectromagnetics. He has published over 280 articles in major refereed journals, nearly 500 conference papers and 20 book chapters. He coauthored the following six books: *Approximate Boundary Conditions in Electromagnetics* (Institution of Electrical Engineers, London, 1995), *Finite Element Method for Electromagnetics* (IEEE Press, New York, 1998), *Frequency Domain Hybrid Finite Element Methods in Electromagnetics* (Morgan & Claypool, 2006), *Computational Methods for High Frequency Electromagnetic Interference* (Verlag, 2009), *Small Antennas* (McGraw-Hill, 2010), and edited the *Antenna Engineering Handbook* (McGraw-Hill, 2007). He has also written several well-edited coursepacks on introductory and advanced numerical methods for electromagnetics, and has delivered short courses on antennas, numerical methods, and frequency selective surfaces.

Dr. Volakis was elected Fellow of the IEEE in 1996, and is a member of the URSI Commissions B and E. In 1998 he received the University of Michigan (UM) College of Engineering Research Excellence award, in 2001 he received the UM, Dept. of Electrical Engineering and Computer Science Service Excellence Award, and in 2010 he received the Ohio State Univ. Clara and Peter Scott award for outstanding academic achievement. He was the 2004 President of the IEEE Antennas and Propagation Society and served on the AdCom of the IEEE Antennas and Propagation Society from 1995 to 1998. He also served as an Associate Editor for the IEEE TRANSACTIONS ON ANTENNAS AND PROPAGATION from 1988–1992, Radio Science from 1994–1997, and for the *IEEE Antennas and Propagation Magazine* (1992–2006), the *J. Electromagnetic Waves and Applications* and the *URSI Bulletin*. He Chaired the 1993 IEEE Antennas and Propagation Society Symposium and Radio Science Meeting in Ann Arbor, MI, and Co-Chaired the same Symposium in 2003 at Columbus, OH. He is listed by ISI among the top 250 most referenced authors. He graduated/mentored nearly 60 Ph.D. students/post-docs, and coauthored with them 14 best paper awards at conferences.